Exomeデータにおける variant call errorのパターン

Monozygotic twins
KUH022&KUH023

KUH022=KUH110927C1
Noonan Syndrome
SS51Mb_v4

KUH023=KUH110927C2
正常表現型
SS80Mb_v4

MZtwin KUH022・KUH023間における塩基置換部位の検索(2013/9/21 KN)

下記の絞り込みは、Noonan syndrome表現型の責任変異絞り込みではなく、KUH022・KUH023間で異なる塩基部位を探すことを目的としている。

###ファイル：2_noonan_1_1_KN2_nd145.txt##########################
RD_KUH022とRD_KUH023が両方とも21以上であるvariantに絞り込み
145 variants

###ファイル：3_noonan_1_1_KN2_nd145andMAF.xslx##########################
さらにminor allele frequencyを計算し、KUH022とKUH023との間でMAFに0.2以上の差があるものに絞り込むと17個のvariantが残る。

このうちの幾つかについてIGVでデータを眺めたところ、in-del周辺の再アライメントの不一致が原因で、KUH022とKUH023とで異なるgenotypeがcallされていると思われる例が認められた。

Chr12:123334929 (hg19)
Chr14:55902698 (hg19)

周辺にin-delが無く、KUH022とKUH023のgenotypeが確かに異なる例もあった。
Chr12:123334929 (hg19)
このような例でも、偶然の偏りの可能性も考えられ、sanger-sequencingによるvalidationが必要と思われる。

Chr14:55902698
(hg19)
ref=T, alt=A
TBPL2 intronic
KUH022: T;A=39;1
KUH023: T;A=15;9

In-del周辺の
Calibration/
re-alignment
エラー例

近傍の2bp insertion
の影響

miss-alignment数が
(おそらく偶然)
偏っている
ために genotype call
不一致

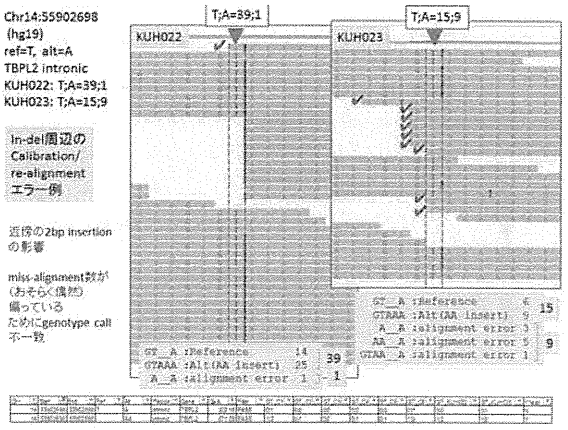

Chr3:101232057 (hg19)
ref=G, alt=A
SENP7 UTR5
AD_KUH022: G;A=23;11
AD_KUH023: G;A= 0;24

一見するとKUH022だけに
に1塩基欠失があるように見える

AAA_AAA
AAAAAA
GAAA
AAA_GAA
AAAG
AAA_GAA
AAAGAAA
などが混在

In-del周辺の
Calibration/
re-alignment
エラー例

実際は下記のパターンか？

KUH022 genotype
AAA_AAA 10
AAAGAAA 29
KUH023 genotype
AAA_AAA 3
AAAGAAA 21

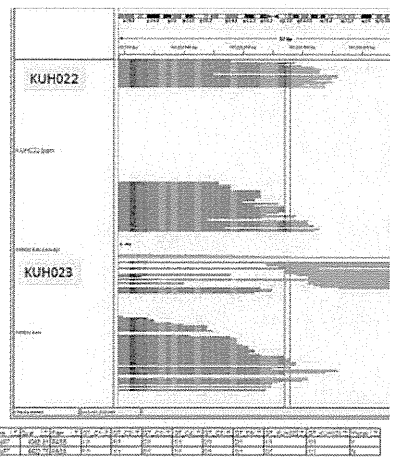

Chr12:123334929 (hg19)
ref=G, alt=T
HIP1R intronic

AD_KUH022: G;T=33;9
AD_KUH023: G;T=22;0

KUH022とKUH023のgenotypeが
確かに異なる例

但し、KUH023でT allele readが
たまたま入ってこなかった可能性
も否定できない

Sanger-sequencingによる
検証が必要

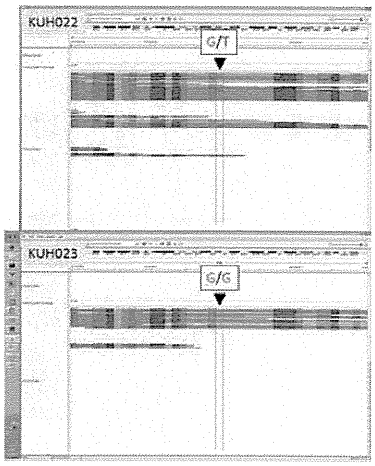

Chr12:123334929 (hg19)
ref=G, alt=T
HIP1R intronic

AD_KUH022: G;T=33;9
AD_KUH023: G;T=22;0

KUH022とKUH023のgenotypeが
確かに異なる例

但し、KUH023でT allele readが
たまたま入ってこなかった可能性
も否定できない

Sanger-sequencingによる
検証が必要

In-del周辺ではcall error
が起きやすいので注意

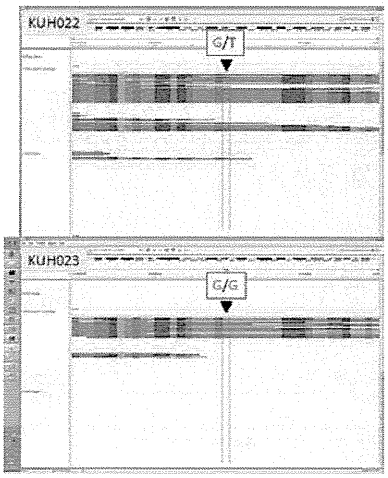

ChIP-qPCR / ChIP条件検討

ChIP-qPCR (SYBR-green 法・ABI7500 使用)　　2013/08/27version　長谷川・中林

準備
↓準備 0: 定量 PCR の測定原理・標準的データ解析原理を理解する。
↓準備 1:　standard curve (検量線) 用断片化 gDNA の準備
↓準備 2: プライマーのデザイン・条件検討
↓準備 3: ChIP DNA・Input DNA 調製
↓準備 4: サンプル (Std, NC, unknown) 配置の決定
↓準備 5: ABI7500software 上で Experiment 作成・保存
↓
PCR 反応セットアップ ⇒ 7500 RUN
↓
測定終了後のデータ評価 (7500software) ⇒ Data Export ⇒ シャットダウン
↓
Excel でのデータ解析

ChIP-qPCR 用定量PCRプライマーの設定(positive regions & negative regions)

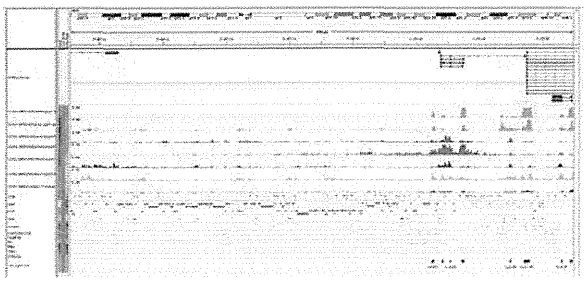

ChIP-qPCR 用定量PCRプライマーの設定(positive regions & negative regions)

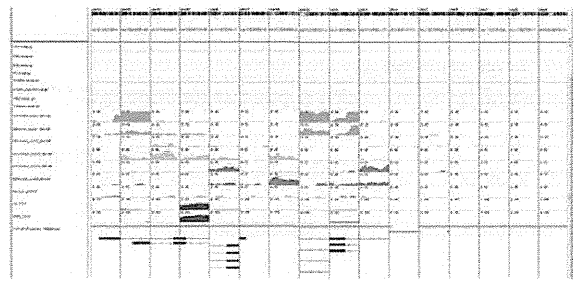

ChIP-qPCR / ChIP条件検討

Check points

end-point PCR産物は単一サイズか？(7500softwareでmelt-curve解析結果を目視確認)

各プライマーについてstandard curveの相関係数Rを確認(AE-calc sheet使用)
各プライマーについてAE算出 (AE-calc sheet使用)

Input-DNA, ChIP-DNAのCt値はstandard curve内に収まっているか？
(negative regionのCt値が外れるのは仕方なし)

Inputのqualityは異なるプライマー間で同程度になるはず

%input=AE^(Ct of input - Ct of ChIP) x Fd x100%
AE: amplification efficiency (fold), ideal value= 2
Fd : cell number of input / cell number of ChIP

%input of Positive Region = AE^(Ct PR of input - Ct PR of ChIP) x Fd x100%

%input of Negative Region = AE^(Ct NR of input - Ct NR of ChIP) x Fd x100%

Relative occupancy
= %input of Positive Region / %input of Negative Region
= (AE^(Ct PR of input - Ct PR of ChIP) x Fd x100%) / (AE^(Ct NR of input - Ct NR of ChIP) x Fd x100%)
= (AE^(Ct PR of input - Ct PR of ChIP)) / (AE^(Ct NR of input - Ct NR of ChIP))

Block 96fast
Chem SYBR GREEN
Exper D:\Applied Biosystems\7500\experiments\mt-biology\Hasegawa\130801 YH.eds
Exper 2013-08-01 18:15:38 PM JST
Instru sds7500fast
Passi ROX

Well	Sample Name	Target Name	Task	Ct	Quantity		%input	Relative occupancy (/N5)	Relative occupancy (/N7)
A1	gDNA C1-C8 mix (sonicaion)_20	GAPDH promoter	STAN	23.76	20.000	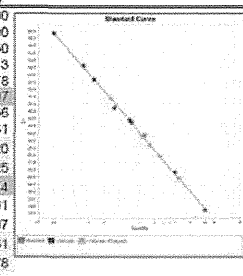			
B1	gDNA C1-C8 mix (sonicaion) 5	GAPDH promoter	STAN	26.36	5.000				
C1	gDNA C1-C8 mix (sonicaion) 5/4	GAPDH promoter	STAN	28.88	1.250				
D1	gDNA C1-C8 mix (sonicaion) 5/16	GAPDH promoter	STAN	30.76	0.313				
E1	gDNA C1-C8 mix (sonicaion) 5/64	GAPDH promoter	STAN	33.67	0.078				
H1	EM0319-2-input_400cells	GAPDH promoter	UNKI	27.47	2.507				
A2	EM0319-2-input_100cells	GAPDH promoter	UNKI	28.82	1.156				
B2	EM0319-2-input_25cells	GAPDH promoter	UNKI	31.42	0.261				
F1	EM0319-2-H3K4me3_50000cells	GAPDH promoter	UNKI	35.86	0.020		0.007%	1.09	0.76
G1	EM0319-2-H3K27ac_50000cells	GAPDH promoter	UNKI	32.70	0.125		0.040%	2.63	2.95
E2	EM0409-input_1000cells	GAPDH promoter	UNKI	25.92	6.074				
F2	EM0409-input_250cells	GAPDH promoter	UNKI	28.25	1.601				
G2	EM0409-input_63cells	GAPDH promoter	UNKI	29.95	0.607				
C2	EM0409-H3K4me3_50000cells	GAPDH promoter	UNKI	29.88	0.631		0.208%	7.87	2.03
D2	EM0409-H3K27ac_50000cells	GAPDH promoter	UNKI	29.75	0.678		0.224%	13.04	4.19
H2	DW	GAPDH promoter	NTC	Undetermi					
A3	gDNA C1-C8 mix (sonicaion)_20	RPL10 promoter	STAN	23.57	20.000	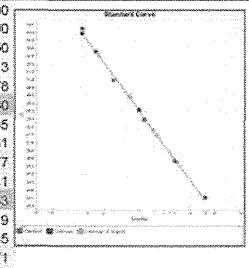			
B3	gDNA C1-C8 mix (sonicaion)_5	RPL10 promoter	STAN	25.86	5.000				
C3	gDNA C1-C8 mix (sonicaion)_5/4	RPL10 promoter	STAN	28.48	1.250				
D3	gDNA C1-C8 mix (sonicaion)_5/16	RPL10 promoter	STAN	30.98	0.313				
E3	gDNA C1-C8 mix (sonicaion)_5/64	RPL10 promoter	STAN	34.27	0.078				
H3	EM0319-2-input_400cells	RPL10 promoter	UNKI	27.80	1.930				
A4	EM0319-2-input_100cells	RPL10 promoter	UNKI	29.93	0.635				
B4	EM0319-2-input_25cells	RPL10 promoter	UNKI	32.55	0.161				
F3	EM0319-2-H3K4me3_50000cells	RPL10 promoter	UNKI	33.95	0.077		0.032%	5.33	3.74
G3	EM0319-2-H3K27ac_50000cells	RPL10 promoter	UNKI	32.80	0.141		0.059%	3.85	4.31
E4	EM0409-input_1000cells	RPL10 promoter	UNKI	25.78	5.553				
F4	EM0409-input_250cells	RPL10 promoter	UNKI	27.51	2.249				
G4	EM0409-input_63cells	RPL10 promoter	UNKI	29.90	0.645				
C4	EM0409-H3K4me3_50000cells	RPL10 promoter	UNKI	29.12	0.971		0.350%	13.22	3.42
D4	EM0409-H3K27ac_50000cells	RPL10 promoter	UNKI	29.08	0.987		0.356%	20.76	6.67
H4	DW	RPL10 promoter	NTC	Undetermi					

ヒストン修飾ChIP-seq例：H3K4me3 & H3K27ac(子宮内膜由来間質細胞)

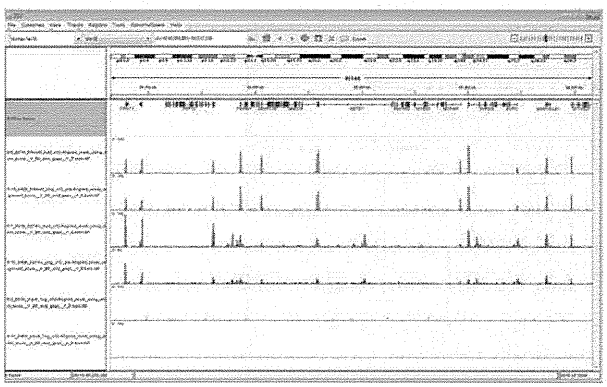

ChIPの最適条件は細胞・ヒストン修飾タイプ・抗体により異なる

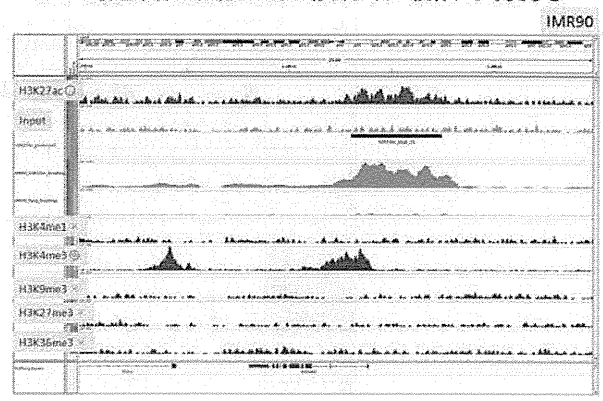

クロマチン調製時に核抽出が必要か？

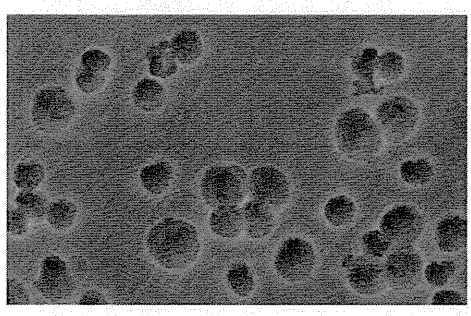

固定細胞はlysis buffer懸濁後も細胞膜がintact

このまま回収するとwhole-cell lysateを回収することになる

細胞膜を何らかの方法で壊すことで、核のみが回収できる。

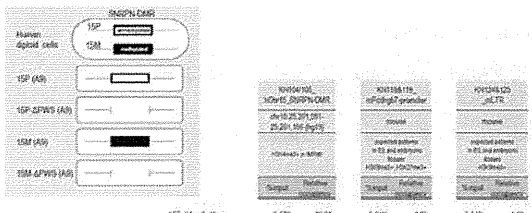

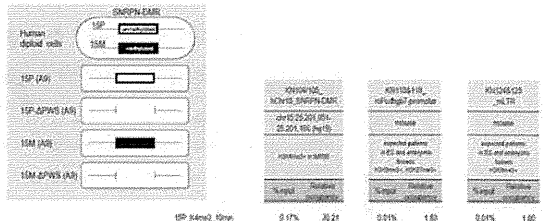

この結果から
核抽出は
不活性化クロマチン修飾ChIP
の特異性を向上させると判断

転写因子のChIP-seq例：免疫系zinc-finger protein (10.5dpc embryo)

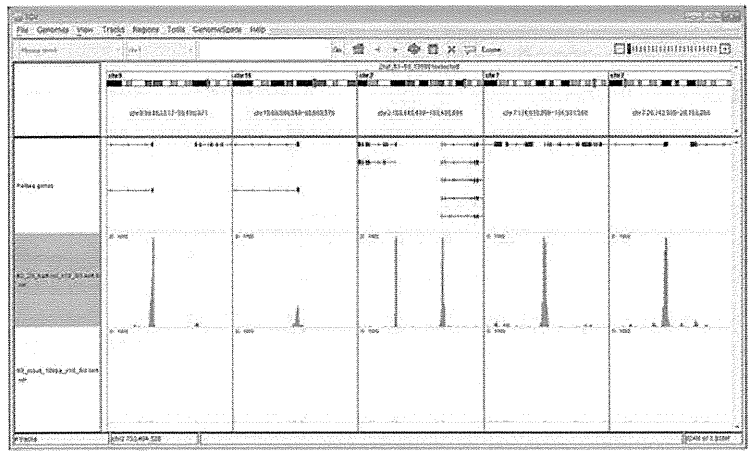

転写因子のChIP-seq例：免疫系zinc-finger protein (10.5dpc embryo)

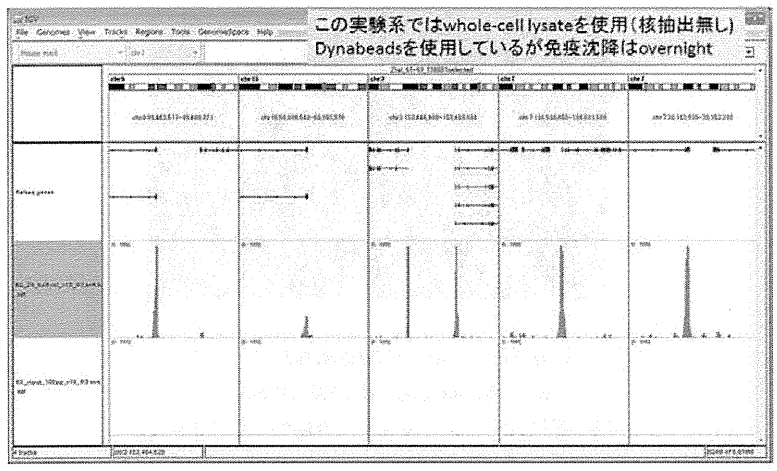

転写因子のChIP-seq例：免疫系zinc-finger protein (10.5dpc embryo)

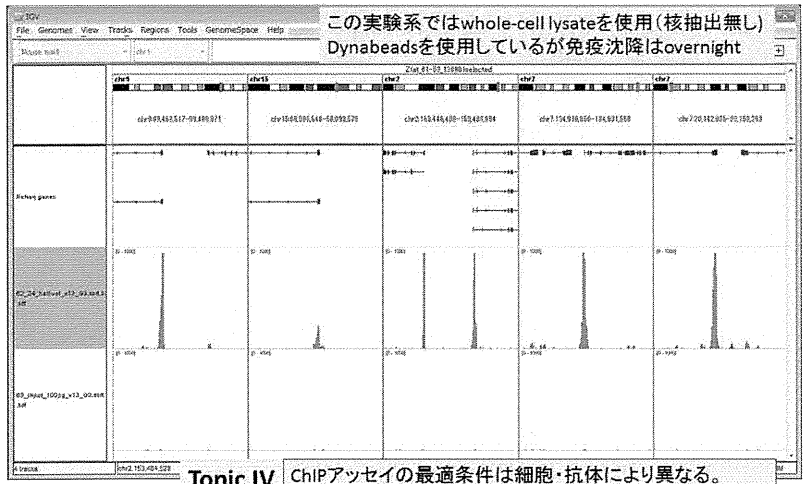

Topic IV

ChIPアッセイの最適条件は細胞・抗体により異なる。

一連の実験条件についての実験者の細心の注意が重要

RRBS

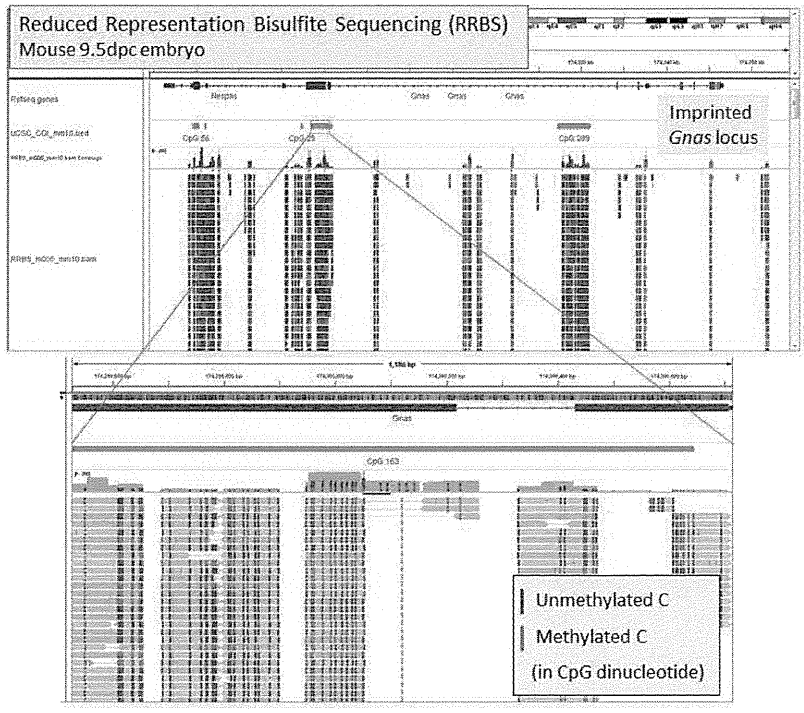
Reduced Representation Bisulfite Sequencing (RRBS)
Mouse 9.5dpc embryo
Imprinted
Gnas locus
Unmethylated C
Methylated C
(in CpG dinucleotide)

厚生労働科学研究費補助金（難病・がん等の疾患分野の医療の実用化研究事業）
分担研究報告書

大規模シークエンスのデータ解析技術の開発および常在細菌叢ゲノムの解析に関する研究

研究分担者　服部 正平　東京大学大学院教授

研究要旨：
本研究は、ヒト腸内細菌叢の細菌組成や遺伝子･機能プロファイル等を解明するための次世代シークエンサーによる大量データに基づいた解析技術を開発し、小児科・産科領域の種々の疾患と腸内細菌叢との関連を解明する。

A．研究目的

本研究は、種々の小児科・産科領域の難治性疾患や稀少疾患の患者の腸内細菌叢等のマイクロバイオームを解析するための次世代シークエンサー（NGS）を用いた大量データの取得と情報科学的解析技術の開発を行い、マイクロバイオームと疾患の関連を解明することを目的とする。

B．研究方法

健常者及び疾患患者の腸内細菌叢等のヒト常在菌叢からNGSを用いて大量の16Sリボソーム RNA 遺伝子（16S）とメタゲノムデータを取得する。ついで、これらの配列データから常在菌叢が有する細菌種・遺伝子・代謝系等の機能特徴を解明する。また、そのための高速で精度の高い情報学解析パイプラインを構築する。

（倫理面への配慮）

本研究ではヒト常在菌の遺伝子情報等を解析する。この遺伝子情報は被験者の遺伝子情報ではないが、個人に固有の情報であるため、法令等により保護される個人情報として取り扱う。そのため、本研究内容について被験者に対して文書と面接による十分な説明（研究の目的、解析データから被験者が特定できない匿名化、個人名が特定されない形式での情報公開、同意後における撤回または継続の中止の容認とそれらのサンプル及び解析結果の廃棄等）を行い、インフォームドコンセントを取得する。よって、解析に供するすべてのサンプルについては、国立成育医療研究センター等の機関の「ヒトゲノム倫理審査委員会」の承認を得た。

C．研究結果

今年度では、初年度から使用しているロシュ社製454GSと2年度目に導入したイオンPGM及びProtonを用いて、ヒト腸内細菌叢の16S及びメタゲノム解析をさらに加速させた。昨年度までに解析した51名日本人健常者に、今年度はさらに49名の被験者を追加し、計100名の成人健常者から腸内細菌叢サンプルを収集した。これらには経時的に得たサンプルも含まれ、最終的に計167サンプルを解析した。また、1歳未満の乳児健常者（7名）、小学生健常者（8名）、重症小児外科疾患患児（14症例）の腸内細菌叢を解析した。

メタゲノム解析では、①計約200Gbの配列データを取得し、約10.8Gbのユニーク配列データを得て、そこから約460万のユニークな遺伝子を情報学的に同定した。②この日本人データセットと公表されている欧米人等の他領域集団のメタゲノムデータを合わせた解析（全1,051サンプル）から、合計約1,100万のユニークな腸内細菌叢遺伝子を同定した。③これらの各地域集団間との比較解析から、各地域集団間の菌種組成が大きく異なることがわかった。例えば、Bifidobacterium属が日本集団ではRuminococcus（あるいはBifidobacterium）属が優占するタイプ1（85%）、Bacteroides属が優占するタイプ2（6%）、Prevotella属が優占するタイプ3（9%）となったが、米国集団では、タイプ1（5%）、タイプ2（88%）、タイプ3（6%）となった。すなわち、各タイプの割合が集団毎に大きく異なり、各タイプが地域集団によって偏りがあることが判明した。④日本人と他の外国地域集団の機能プロファイルの比較解析か

ら、日本人集団にのみ特徴的で有意に多い機能（539 遺伝子）と少ない機能（116 遺伝子）を同定した。多い機能には炭水化物代謝系（特に、PTS と酢酸生合成）やアミノ酸代謝系が顕著であり、少ない機能には膜合成系や DNA 修復系が含まれている。これらの日本人集団に多い機能の大部分が Bifidobacterium 由来の遺伝子であることがわかった。その中で、グルタミン酸トランスポーターやグルカン分解酵素等は日本人特有の食文化との関連が示唆される。一方で日本人集団に特徴的に少ない菌種・遺伝子機能として、メタン生成の代謝系と古細菌(Methanobrevibacter)の関係を明らかにした。

16S 遺伝子解析では、16S 遺伝子を増幅する PCR プライマーの改良や情報解析の条件最適化、人工細菌叢を用いた総合的な定量評価等からきわめて定量性の高い 16S 解析システムを開発した。この解析システムを用いた 1 歳未満の乳児（7 名）と小学生健常者（8 名）の 16S 遺伝子解析から、小学生）の細菌叢では成人と同程度の菌種と菌種組成が検出された。一方、1 歳未満の離乳前乳児の腸内細菌叢には成人よりも少ない数の菌種が検出され、その菌種組成も大きく成人と異なっていた。これらの結果は、離乳前乳児の腸内細菌叢は離乳後に急速に成人型へと成熟することを示す。重症小児外科疾患患児（短腸症、腹壁破裂、ヒルシュスプルング症等）に対して治療的シンバイオティクス療法を施行した 7 例と生後早期から予防的シンバイオティクス療法を施行した 7 例の腸内細菌叢（糞便）を 16S 遺伝子解析した。解析した 14 例中、投与した Bifidobacterium breve 菌は検出されることが多いが Lactobacillus casei 菌はほとんど検出されなかった。また、治療的シンバイオティクス療法を施行した 7 症例では細菌叢の多様性が失われており、プロバイオティクス療法試行中のサンプルにもかかわらず Lactobacillus 等の好気性菌の増加が目立った。一方、予防的シンバイオティクス療法を施行した症例では細菌叢の多様性がみられ Bifidobacterium 属が優占することが明らかになった。

D．考察

確立した次世代シークエンサー操作と情報学的解析手法を駆使した成人健常者の日本と外国サンプル（総数 1,000 名以上）の解析から、日本人集団を含め地域集団の腸内細菌叢の菌叢構造とその機能プロファイルが有意に多様化していることを見出した。この結果は腸内細菌叢が人種の分岐後、それぞれ独自に進化・形成されたことを示唆する。しかし、この地域集団間の細菌叢多様性は必ずしも宿主のヒトの遺伝的距離とは相関せず、また、食習慣だけでも説明できない。つまり、ヒト集団に形成される腸内細菌叢の形成機構には、上記を含めた様々な要因が複雑に関与していると考えられる。よって、腸内細菌叢が関係する様々な疾患の研究には、この地域集団間における腸内細菌叢構造及び機能の違いを考慮する必要がある。

乳児及び小学生の解析から、誕生初期の細菌叢は不安定で未成熟であるが、離乳後に急速に安定した成人細菌叢へと変わっていくことが示唆される。重症小児外科疾患患児の治療的シンバイオティクス療法群は、今回の解析からその異常細菌叢を正常に近い形に誘導することが難しいことが判明した。一方、予防的シンバイオティクス療法群では、投与した Bifidobacterium 菌が優占した菌叢を維持しており、早期の腸内細菌叢コントロールが正常腸内細菌叢誘導には極めて重要であることが示唆された。また、プロバイオティクスとして投与された Lactobacillus casei 菌はいずれの群でも腸内細菌叢中にはほとんど検出されず、この菌の投与の意義については今後検討する必要があると考えられた。

E．結論

この最終年度では、開発したヒト腸内細菌叢の解析手法の有効性とデータ精度の高度化を証明できた。この技術を用いて、ヒト腸内細菌叢の菌叢構造及び機能プロファイルがヒトの地域集団で有意に異なることを発見した。また、消化器系の重症小児の腸内細菌叢の解析と予防的・治療的シンバイオティクス療法の評価を本解析法を用いて行った。これらの成果は、今後、常在細菌叢を用いたあるいはターゲットとした新規な寛解法や治療法の開発に繋がると期待できる。

F．健康危険情報

なし

G．研究発表

1．論文発表

Kim SW 他：Robustness of gut microbiota of healthy adult in response to probiotic intervention revealed by high-throughput pyrosequencing. DNA Res. 20(3): 241-253 (2013).

Said HS 他：Dysbiosis of salivary microbiota in inflammatory bowel disease and its association with oral immunological biomarkers. DNA Res. 21(1): 15-25 (2013).

Atarashi K 他：Treg induction by a rationally selected mixture of Clostridia strains from the human microbiota. Nature 500(7461): 232-236 (2013).

Yoshimoto S 他：Obesity-induced gut microbial metabolite promotes liver cancer through senescence secretome. Nature 499(7456): 97-101 (2013).

Toh H 他：Genomic adaptation of the Lactobacillus casei group. PLoS One. 8(10): e75073 (2013).

Song S 他：Our second genome - Human Metagenome - How next generation sequencer changes our life through microbiology. Adv. Microb. Physiol. 62: 119-144 (2013).

2. 学会発表

服部正平：ヒト腸内細菌叢の多様性と解析法の進歩．第 41 回日本臨床免疫学会(招待講演)（平成 25 年 11 月）。

服部正平：次世代シークエンサーが読み解くヒトマイクロバイオーム．第 41 回糸球体障害研究会（招待講演）(平成 25 年 11 月)。

西嶋傑, 服部正平他: Comparative metagenomics of Japanese and European gut microbiomes. (The Biology of Genomes, ポスター発表)（平成 25 年 5 月）。

H．知的財産権の出願・登録状況

1. 取得特許

なし

2. 実用新案登録

なし

3. その他

なし

III. 研究成果の刊行に関する一覧表

研究成果の刊行に関する一覧表

雑誌

発表者氏名	論文タイトル名	発表誌名	巻号	ページ	出版年
Nakamura K, Aizawa K, Nakabayashi K, Kato N, Yamauchi J, Hata K, Tanoue A.	DNA methyltransferase inhibitor zebularine inhibits human hepatic carcinoma cells proliferation and induces apoptosis.	PLoS One	8(1)	e54036	2013
Iglesias-Platas I, Martin-Trujillo A, Cirillo D, Court F, Guillaumet-Adkins A, Camprubi C, Bourc'his D, Hata K, Feil R, Tartaglia G, Arnaud P, Monk D.	Characterization of novel paternal ncRNAs at the Plagl1 locus, including Hymai, predicted to interact with regulators of active chromatin.	PLoS One	7(6)	e38907	2012
Higashimoto K, Nakabayashi K, Yatsuki H, Yoshinaga H, Jozaki K, Okada J, Watanabe Y, Aoki A, Shiozaki A, Saito S, Koide K, Mukai T, Hata K, Soejima H.	Aberrant methylation of H19-DMR acquired after implantation was dissimilar in soma versus placenta of patients with Beckwith-Wiedemann syndrome.	Am J Med Genet A.	158A(7)	1670-1675	2012
Kobayashi H, Sakurai T, Sato S, Nakabayashi K, Hata K, Kono T.	Imprinted DNA methylation reprogramming during early mouse embryogenesis at the Gpr1-Zdbf2 locus is linked to long cis-intergenic transcription.	FEBS Lett	586(6)	827-833	2012
Nakanishi MO, Hayakawa K, Nakabayashi K, Hata K, Shiota K, Tanaka S.	Trophoblast-specific DNA methylation occurs after the segregation of the trophectoderm and inner cell mass in the mouse periimplantation embryo.	Epigenetics.	7(2)	173-182	2012
Kobayashi H, Sakurai T, Imai M, Takahashi N, Fukuda A, Yayoi O, Sato S, Nakabayashi K, Hata K, Sotomaru Y, Suzuki Y, Kono T.	Contribution of intragenic DNA methylation in mouse gametic DNA methylomes to establish oocyte-specific heritable marks.	PLoS Genet	8(1)	e1002440	2012
Kim SW, Suda W, Kim S, Oshima K, Fukuda S, Ohno H, Morita H, Hattori M.	Robustness of gut microbiota of healthy adults in response to probiotic intervention revealed by high-throughput pyrosequencing.	DNA Res	20(3)	241-253	2013

発表者氏名	論文タイトル名	発表誌名	巻号	ページ	出版年
Said HS, Suda W, Nakagome S, Chinen H, Oshima K, Kim S, Kimura R, Iraha A, Ishida H, Fujita J, Mano S, Morita H, Dohi T, Oota H, Hattori M.	Dysbiosis of salivary microbiota in inflammatory bowel disease and its association with oral immunological biomarkers.	DNA Res.	21(1)	15-25	2014
Atarashi K, Tanoue T, Oshima K, Suda W, Nagano Y, Nishikawa H, Fukuda S, Saito T, Narushima S, Hase K, Kim S, Fritz JV, Wilmes P, Ueha S, Matsushima K, Ohno H, Olle B, Sakaguchi S, Taniguchi T, Morita H, Hattori M, Honda K.	Treg induction by a rationally selected mixture of Clostridia strains from the human microbiota.	Nature	500 (7461)	232-236	2013
Yoshimoto S, Loo TM, Atarashi K, Kanda H, Sato S, Oyadomari S, Iwakura Y, Oshima K, Morita H, Hattori M, Honda K, Ishikawa Y, Hara E, Ohtani N.	Obesity-induced gut microbial metabolite promotes liver cancer through senescence secretome.	Nature	499 (7456)	97-101	2013
Toh H, Oshima K, Nakano A, Takahata M, Murakami M, Takaki T, Nishiyama H, Igimi S, Hattori M, Morita H.	Genomic adaptation of the Lactobacillus casei group.	PLoS One	8(10)	e75073	2013

IV. 研究成果の刊行物・別刷

OPEN ACCESS Freely available online

PLOS | ONE

DNA Methyltransferase Inhibitor Zebularine Inhibits Human Hepatic Carcinoma Cells Proliferation and Induces Apoptosis

Kazuaki Nakamura[1]*, Kazuko Aizawa[1], Kazuhiko Nakabayashi[2], Natsuko Kato[1], Junji Yamauchi[1], Kenichiro Hata[2], Akito Tanoue[1]

1 Department of Pharmacology, National Research Institute for Child Health and Development, Tokyo, Japan, **2** Department of Maternal-Fetal Biology, National Research Institute for Child Health and Development, Tokyo, Japan

Abstract

Hepatocellular carcinoma is one of the most common cancers worldwide. During tumorigenesis, tumor suppressor and cancer-related genes are commonly silenced by aberrant DNA methylation in their promoter regions. Zebularine (1-(β-$_D$-ribofuranosyl)-1,2-dihydropyrimidin-2-one) acts as an inhibitor of DNA methylation and exhibits chemical stability and minimal cytotoxicity both *in vitro* and *in vivo*. In this study, we explore the effect and possible mechanism of action of zebularine on hepatocellular carcinoma cell line HepG2. We demonstrate that zebularine exhibits antitumor activity on HepG2 cells by inhibiting cell proliferation and inducing apoptosis, however, it has little effect on DNA methylation in HepG2 cells. On the other hand, zebularine treatment downregulated CDK2 and the phosphorylation of retinoblastoma protein (Rb), and upregulated $p21^{WAF/CIP1}$ and p53. We also found that zebularine treatment upregulated the phosphorylation of p44/42 mitogen-activated protein kinase (MAPK). These results suggest that the p44/42 MAPK pathway plays a role in zebularine-induced cell-cycle arrest by regulating the activity of $p21^{WAF/CIP1}$ and Rb. Furthermore, although the proapoptotic protein Bax levels were not affected, the antiapoptotic protein Bcl-2 level was downregulated with zebularine treatment. In addition, the data in the present study indicate that inhibition of the double-stranded RNA-dependent protein kinase (PKR) is involved in inducing apoptosis with zebularine. These results suggest a novel mechanism of zebularine-induced cell growth arrest and apoptosis via a DNA methylation-independent pathway in hepatocellular carcinoma.

Citation: Nakamura K, Aizawa K, Nakabayashi K, Kato N, Yamauchi J, et al. (2013) DNA Methyltransferase Inhibitor Zebularine Inhibits Human Hepatic Carcinoma Cells Proliferation and Induces Apoptosis. PLoS ONE 8(1): e54036. doi:10.1371/journal.pone.0054036

Editor: William B. Coleman, University of North Carolina School of Medicine, United States of America

Received September 18, 2012; **Accepted** December 7, 2012; **Published** January 8, 2013

Funding: This work was supported in part by research grants from the Takeda Science Foundation (Osaka, Japan, http://www.takeda-sci.or.jp/index.html), and The Grant of National Center for Child Health and Development (22A–6) (Tokyo, Japan, http://www.ncchd.go.jp/index.php). The funders had no role in study design, data collection and analysis, decision to publish, or preparation of the manuscript.

Competing Interests: The authors have declared that no competing interests exist.

* E-mail: nakamura-kz@ncchd.go.jp

Introduction

Hepatocellular carcinoma (HCC) is the sixth most common newly diagnosed cancer and the third most common cause of cancer mortality worldwide. Its treatment outcome is far from satisfactory and the five-year survival rate is dismal (approximately 10%) [1]. Liver transplantation is currently considered to be the only curative therapy. Unfortunately, however, a majority (>80%) of patients with advanced and unresectable HCC are not suitable candidates for transplantation or surgical resection [2,3]. Chemotherapy using conventional cytotoxic drugs, such as doxorubicin, cisplatin, and fluorouracil, is a common treatment option, especially for patients with unresectable tumors. However, because of poor response rates, severe toxicities, and high recurrence rates, the mean survival time is approximately six months [3,4]. Thus, there is a very high demand for more effective agents to better combat this malignancy.

It has been considered that hypermethylation of CpG islands in tumor suppressor genes represents one of the hallmarks in human cancer development [5,6]. It has been reported that the analysis of gene expression and promoter CpG island hypermethylation in HCC revealed that both genetic and epigenetic changes contribute to the initiation and progression of liver cancer and are correlated with poor survival [7]. Epigenetic changes such as DNA methylation are pharmacologically reversible, and this offers a promising multi-target translational strategy against cancer in which the expression of a variety of silenced genes could be reactivated. DNA methylation is specifically mediated by the action of DNA methyltransferase (DNMT) enzymes [8], which includes DNMT1, DNMT2, DNMT3a, and DNMT3b [9]. DNMT1 has de novo as well as maintenance methyltransferase activity, and DNMT3a and DNMT3b are potent de novo methyltransferase [10]. Overexpression of DNMT has been reported to be involved in tumorigenesis [11] and has been suggested as a prognostic factor in large B cell lymphomas [12]. Therefore, it has been proposed that the inhibition of DNMT activity can strongly reduce the formation of tumors [13]. Thus far, three DNMT-inhibiting cytosine nucleoside analogs (i.e., 5′-azacitidine, decitabine, and zebularine) have been studied as potential anti-cancer drugs [14–16]. Decitabine and its prodrug 5′-azacitidine are two widely used DNMT inhibitors for the

treatment of patients with various cancers, such as myelodysplastic syndromes (MDS) and acute myeloid leukemia (AML) [17,18]. Although Decitabine and its prodrug 5′-azacitidine are effective in treating various cancers [17,18], the formation of irreversible covalent adducts with DNA may cause long-term side effects, including DNA mutagenesis, a potential cause of tumor recurrence.

Zebularine is a second-generation, highly stable hydrophilic inhibitor of DNA methylation with oral bioavailability that preferentially targets cancer cells [19], as demonstrated in bladder, prostate, lung, colon, and pancreatic carcinoma cell lines [20]. It acts primarily as a trap for DNMT protein by forming tight covalent complexes between DNMT protein and zebularine-substitute DNA [21]. Zebularine is also a cytidine analog that was originally developed as a cytidine deaminase inhibitor. It exhibits low toxicity in mice, even after prolonged administration [22–24]. Given that aberrant methylation is a major event in the early and late stages of tumorigenesis [25,26], including hepatocarcinogenesis [7], this process may represent a critical target for cancer risk assessment, treatment, and chemoprevention [19]. In the previous study, a zebularine signature that classified liver cancer cell lines into two major subtypes with different drug response was identified. In drug-sensitive cell lines, zebularine caused inhibition of proliferation coupled with increased apoptosis, whereas drug-resistant cell lines were associated with the upregulation of oncogenic networks (e.g., E2F1, MYC, and TNF) [19]. However, little is known about the anti-cancer effect and possible mechanism of action of zebularine on HCC.

In the present study, we investigated the molecular mechanism of zebularine against HCC. We demonstrated that zebularine exhibited antitumor activity by inhibiting cell proliferation and inducing apoptosis. This effect was independent of DNA methylation, and characterized by the downregulation of CDK2 and the phosphorylation of retinoblastoma protein (Rb) as well as the upregulation of $p21^{WAF/CIP1}$ and p53. We also found that zebularine induced apoptosis though the intrinsic and extrinsic apoptosis pathways. In addition, the data in the present study suggest that the inhibition of the double-stranded RNA-dependent protein kinase (PKR) is involved in inducing apoptosis with zebularine.

Materials and Methods

Cell culture

HepG2 cells (JCRB1054) and HeLa cells (JCRB9004) were purchased from the Health Science Research Resources Bank (Japan Health Sciences Foundation, Osaka, Japan), and were maintained at 37°C under an atmosphere of 95% air and 5% CO_2 in Dulbecco's modified Eagle's medium (DMEM) containing 10% fetal bovine serum (FBS), 100 U/ml penicillin, and 100 μg/ml streptomycin. Cells were immersed in a culture medium containing the indicated zebularine concentrations. Zebularine (Wako Pure Chemical Industries, Osaka, Japan) was dissolved in distilled water as a stock solution.

Cell viability assay

The cell viabilities after exposure to zebularine were determined using WST assay. The assay was performed using a Cell Counting Kit-8 (Dojindo Laboratories, Kumamoto, Japan) according to the manufacturer's instructions. Cell cultures exposed to 0 μM zebularine were considered to be 100% viable. The cell viability of each drug-treated sample was presented as a percentage of the viability of cultures treated with 0 μM zebularine. All samples were run five times in the same assay.

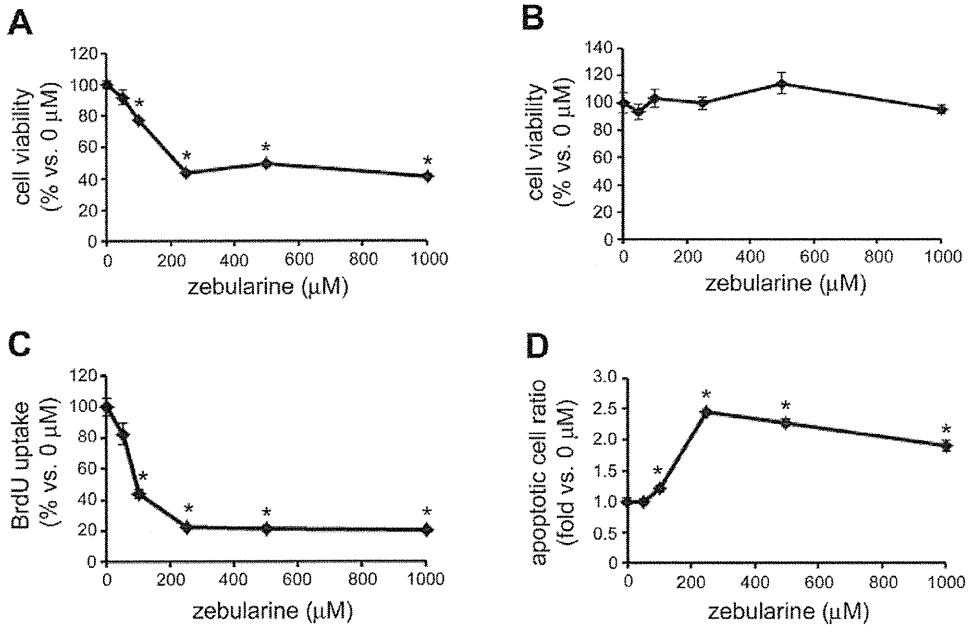

Figure 1. The effect of zebularine on HepG2 cell viability. HepG2 cells were treated with zebularine at indicated concentrations for 72 h (A) and 24 h (B). Cell growth was measured by WST assay. (C) HepG2 cells were treated with zebularine at indicated concentrations for 24 h. Uptake of BrdU was measured by ELISA. (D) HepG2 cells were treated with zebularine at indicated concentrations for 72 h. Apoptosis was measured by TUNEL assay. Data are the means ± SEM of results from at least three independent experiments. *$p<0.05$, compared to 0 μM.
doi:10.1371/journal.pone.0054036.g001

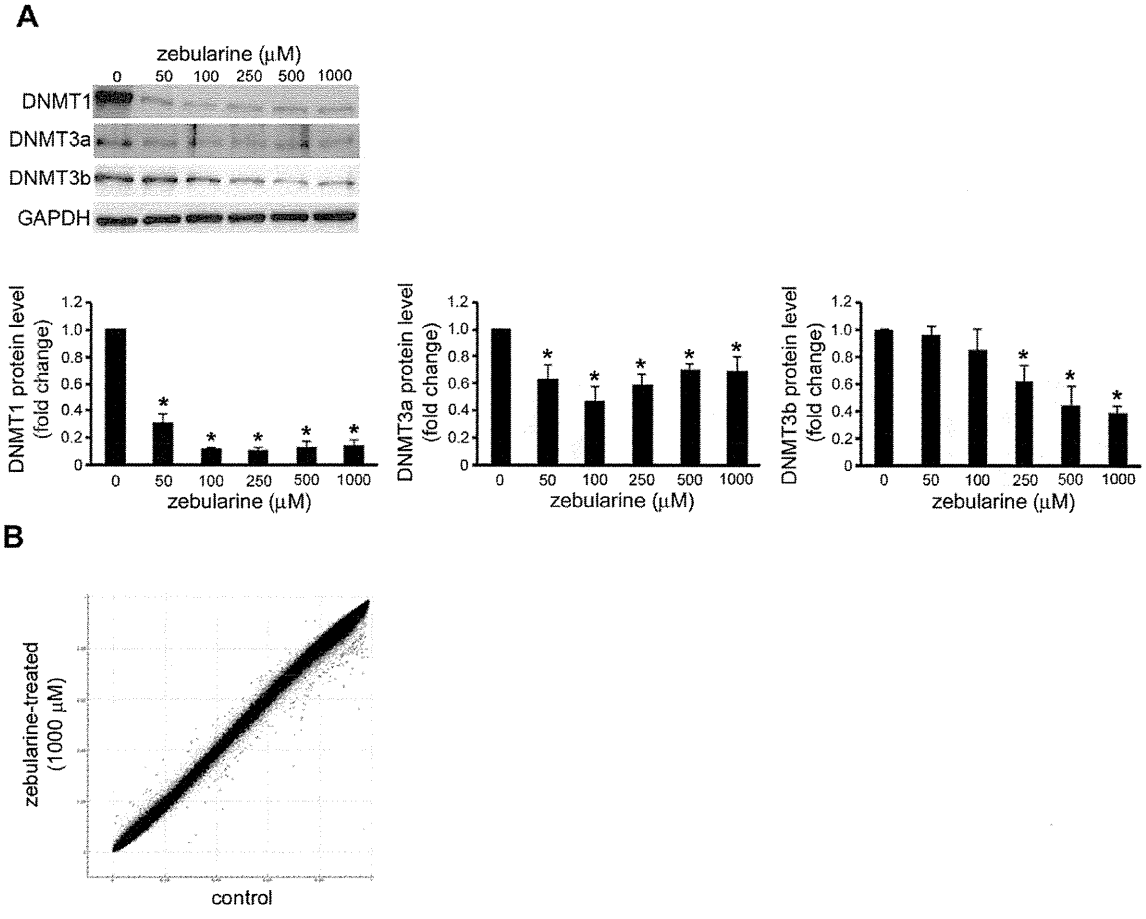

Figure 2. Effect of zebularine on the DNMTs expression and DNA methylation in HepG2 cells. (A) The protein level of DNMT1, DNMT3a, and DNMT3b after zebularine treatment for 72 h at different concentrations. After treatment, the cells were harvested and western blot analysis was performed to detect the protein level of DNMT1, DNMT3a, and DNMT3b. GAPDH was used as a loading control. Data are the means ± SEM of results from at least three independent experiments. *$p<0.05$, compared to 0 μM. (B) Scatter plot of the average beta values at 485,415 CpG sites for zebularine-treated (y-axis) and control (x-axis) HepG2 cells (n = 3 for each group). Dots for CpG sites whose delta-beta value is >0.1 or <−0.1 are shown in green (35 [0.0072%] hypermethylated and 162 [0.033%] hypomethylated CpG sites).
doi:10.1371/journal.pone.0054036.g002

Apoptosis analysis

Quantification of apoptotic cells was performed using a Cell Death Detection ELISA^{PLUS} (Roche Diagnostics, Tokyo, Japan). After 72 h of incubation with zebularine, cells were lysed with a lysis buffer (included in the kit). The assay was performed according to the manufacturer's instructions. Absorbance values were measured at 405 nm using a microplate reader (ARVO, PerkinElmer Japan, Kanagawa, Japan). The apoptotic ratio of each drug-treated sample was presented as a fold-change of the apoptosis of cultures treated with 0 μM zebularine. All samples were run five times in the same assay.

5-bromo-2′-deoxy-uridine (BrdU) incorporation assay

Cellular DNA synthesis rates were determined by measuring BrdU incorporation with the commercial Cell Proliferation ELISA System (Roche Diagnostics). After 24 h of incubation with zebularine, cells were incubated for 3 h with a BrdU labeling solution (included in the kit) containing 10 μM BrdU. The assay was performed according to the manufacturer's instructions. Absorbance values were measured at 405 nm using a microplate reader. The BrdU incorporation of each drug-treated sample was presented as a percentage of the BrdU incorporation of cultures treated with 0 μM zebularine. All samples were run five times in the same assay.

Illumina Infinium HumanMethylation450 BeadChip analysis

Genomic DNA was extracted from three independent cell culture batches for zebularine (1000 μM)-treated and control HepG2 cells. Genomic DNA (1000 ng) was bisulfite-treated and purified using the EpiTect Bisulfite Plus Kit (QIAGEN K.K., Tokyo, Japan). Three hundred nanograms of bisulfite-treated DNA were hybridized to the Illumina Infinium HumanMethylation450 BeadChip using Illumina-supplied reagents and protocols. Both the CpG loci included on this array and the technologies behind the platform have been described previously [27]. GenomeStudio software (Illumina) was used to calculate the methylation level at each CpG site as beta value (β = intensity of the methylated allele [M]/[intensity of the unmethylated allele (U)

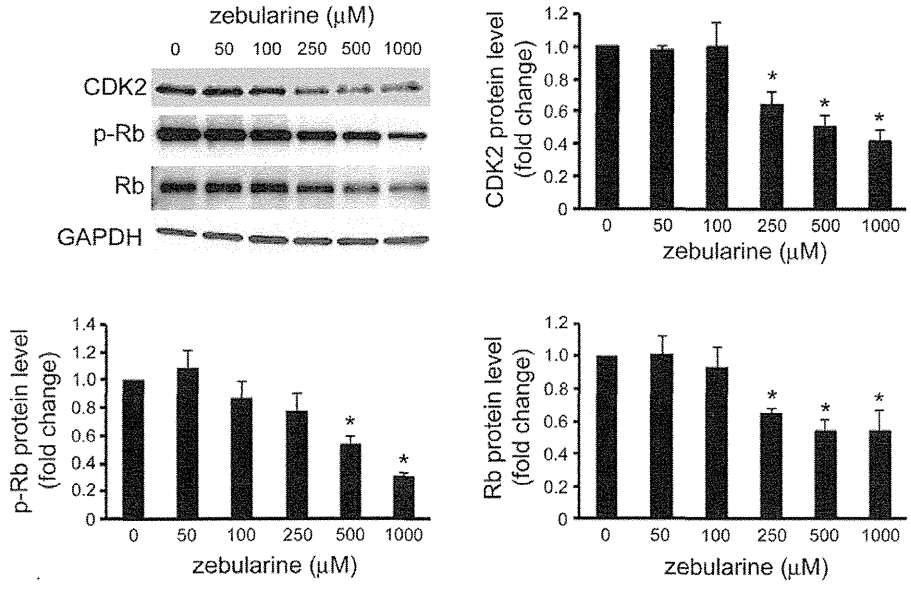

Figure 3. Effects of zebularine on the protein expression of cell-cycle regulator. The protein level of CDK2, p-Rb, and Rb after zebularine treatment for 24 h at different concentrations. After treatment, the cells were harvested and western blot analysis was performed to detect the protein level of CDK2, p-Rb, and Rb. GAPDH was used as a loading control. Data are the means ± SEM of results from at least three independent experiments. *$p<0.05$, compared to 0 μM.
doi:10.1371/journal.pone.0054036.g003

+ intensity of the methylated allele (M) + 100]) [27]. Region-level methylation analysis was conducted using the IMA package [28].

Caspase assays

Caspase-3/7, -8, and -9 activities were assayed with Caspase-Glo Assays (Promega KK, Tokyo, Japan) according to the respective manufacturer's standard cell-based assay protocol. The luminescence of each sample was measure using a plate-reading luminometer. Comparison of the luminescence from a treated sample with a control sample enables determination of the relative increase in caspase activity. All samples were run five times in the same assay.

Overexpression of PKR and forward transfection

The PKR plasmid, pFN21A-hPKR (pFN21AE2332), and empty vector, HaloTag control vector, were purchased from Promega. Transient transfection in HepG2 cells was performed according to the Lipofectamine 2000 (Invitrogen, LifeTechnologies Japan, Tokyo, Japan) methods. Cells cultured in a six-well culture plate were washed twice with phosphate-buffered saline and the medium was replaced with 2 ml of Opti-MEM (Invitrogen) with 1% FBS. Two micrograms per well of pFN21A-hPKR or the empty vector (HaloTag control vector) were then mixed with 10 μl/well of Lipofectamine 2000 in Opti-MEM and the mixture was added to the wells 20 min later. After 6 h of transfection, the cells were then cultured in regular medium for 48 h and subsequently treated with zebularine for 72 h.

Immunoblotting

Cells were lysed in lysis buffer (20 mM HEPES-NaOH pH 7.5, 150 mM NaCl, 1% NP-40, 1.5 mM MgCl2, 1 mM EGTA, 1 μg/ml leupeptin, 1 mM PMSF, and 1 mM Na_3VO_4) and stored at −80°C until use. After centrifugation, aliquots of the supernatants underwent sodium dodecyl sulfate polyacrylamide gel electrophoresis (SDS-PAGE). The electrophoretically separated proteins were transferred to polyvinylidene fluoride (PVDF) membranes, blocked, and immunoblotted with anti-CDK2 (78B2, #2546), Rb (4H1, #9309), phospho-Rb (Ser807/811) (#9308), $p21^{WAF/CIP1}$

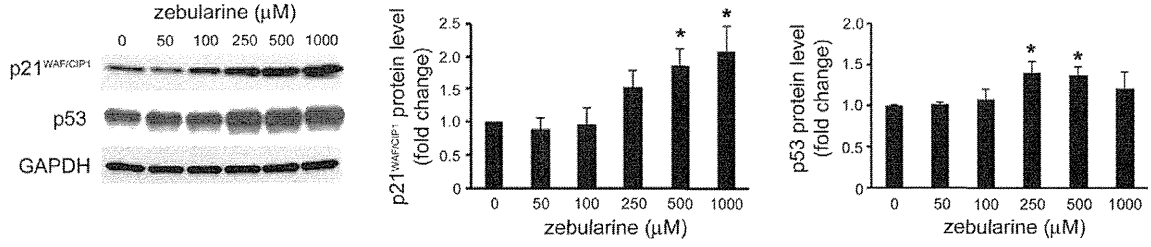

Figure 4. Effects of zebularine on the protein expression of $p21^{WAF/CIP1}$ and p53. The expression of $p21^{WAF/CIP1}$ and p53 after zebularine treatment for 24 h at different concentrations. After treatment, the cells were harvested and western blot analysis was performed to detect the protein level of $p21^{WAF/CIP1}$ and p53. GAPDH was used as a loading control. Data are the means ± SEM of results from at least three independent experiments. *$p<0.05$, compared to 0 μM.
doi:10.1371/journal.pone.0054036.g004

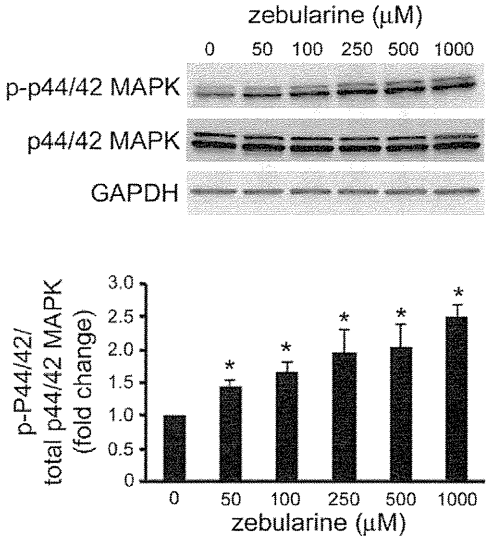

Figure 5. Effects of zebularine on phosphorylation of p44/42 MAPK. The phosphorylation and expression of p44/42 MAPK after zebularine treatment for 24 h at different concentrations. After treatment, the cells were harvested and western blot analysis was performed to detect the phosphorylated and total p44/42 MAPK protein level. GAPDH was used as a loading control. Data are the means ± SEM of results from at least three independent experiments. *$p<0.05$, compared to 0 μM.
doi:10.1371/journal.pone.0054036.g005

(12D1, #2947), p44/42 mitogen-activated protein kinase (MAPK) (137F5, #4695), phospho-p44/42 MAPK (The202/Thy204) (#4370), Bax (D2E11, #5023), Bcl-2 (50E3, #2870), PKR (N216, #2766), DNMT1 (D63A6, #5032) (Cell Signaling Technology Japan, Tokyo, Japan), phospho-PKR (E120, ab32036, abcam, Tokyo, Japan), p53 (M 7001, Dako Japan, Tokyo, Japan), DNMT3a (sc-20703), DNMT3b (sc-81252) (Santa Cruz Biotechnology, Santa Cruz, CA), or glyceraldehyde 3-phosphate dehydrogenase (GAPDH) (#MAB374, Millipore, Temecula, CA) antibodies, and then with peroxidase-conjugated secondary antibodies (NA931 or NA940, GE Healthcare Japan, Tokyo, Japan). The bound antibodies were detected using the ECL system (GE Healthcare Japan).

Statistics

All experiments were performed at least three times. Values are expressed as means ± standard error of the mean (SEM). Statistical analyses were performed using an unpaired Student's *t*-test or two-way analysis of variance (ANOVA) followed by Fisher's protected least significant difference as a post-hoc test. $p<0.05$ was considered to indicate statistical significance.

Results

The effects of zebularine on HepG2 cell viability

In order to investigate the effect of zebularine on HepG2 cell viability, we performed WST assay after zebularine exposure. WST assay indicated that zebularine affected cell viability. Exposure of cells to zebularine for 72 h resulted in a decrease in cell viability (Fig. 1A). To further determine whether zebularine could inhibit the proliferation of HepG2 cells, we conducted BrdU incorporation assay after zebularine treatment for 24 h. Although WST assay indicated that zebularine could not affect cell viability after 24 h (Fig. 1B), BrdU incorporation assay clearly showed that the uptake of BrdU by HepG2 cells was already reduced after 24 h exposure to zebularine (Fig. 1C). At a concentration of 250 μM, the uptake of BrdU was reduced to 22.1±0.6% compared with 0 μM and a similar reduction of BrdU uptake (20.1±1.5%) was observed at a concentration of 1000 μM. In addition, we examined whether zebularine could induce HepG2 cell death. Terminal deoxynucleotidyl transferase dUTP nick end labeling

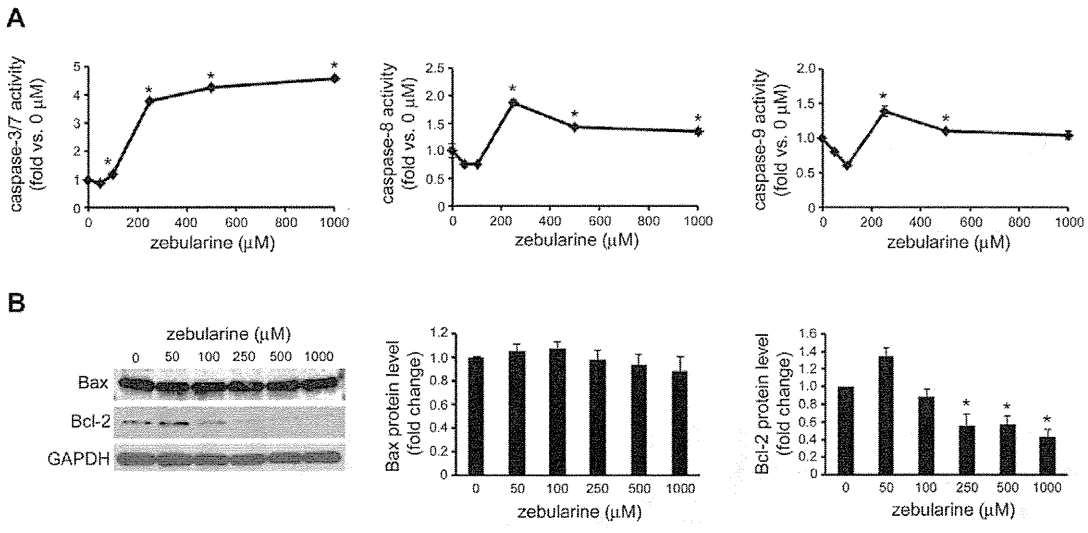

Figure 6. The effect of zebularine on apoptosis-related proteins. HepG2 cells were treated with zebularine at indicated concentrations for 72 h. (A) Caspase-3/7, -8, and -9 activities were determined using Caspase-Glo Assays. The data are expressed as fold-increase relative to the respective untreated samples (RLU/60 min/μg protein). (B) The protein level of Bax and Bcl-2 after zebularine treatment for 72 h at different concentrations. After treatment, the cells were harvested and western blot analysis was performed to detect the protein level of Bax and Bcl-2. GAPDH was used as a loading control. Data are the means ± SEM of results from at least three independent experiments. *$p<0.05$, compared to 0 μM.
doi:10.1371/journal.pone.0054036.g006

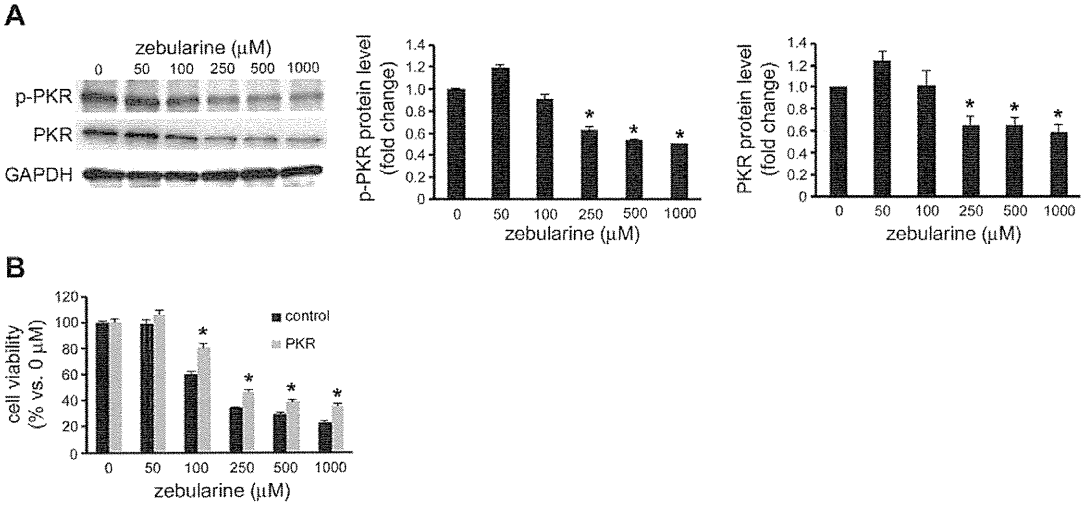

Figure 7. Effects of zebularine on phosphorylation of PKR. (A) The phosphorylation and expression of PKR after zebularine treatment for 72 h at different concentrations. After treatment, the cells were harvested and western blot analysis was performed to detect the phosphorylated and total PKR protein level. GAPDH was used as a loading control. *$p<0.05$, compared to 0 μM. (B) Effect of the overexpression of PKR in zebularine-induced cell death. The forward transfection of the empty vector (Halo Tag control vector) as the control or the plasmid-containing PKR cDNA sequence (pFN21A-hPKR) was performed, and the cells were then treated with different concentrations of zebularine for 72 h. *$p<0.05$, compared to control. Data are the means ± SEM of results from at least three independent experiments.
doi:10.1371/journal.pone.0054036.g007

(TUNEL) assay demonstrated that zebularine induced apoptotic cell death on HepG2 cells. Exposure of cells to zebularine for 72 h resulted in an increase in the number of apoptotic cells (Fig. 1D). These results indicated that DNA replication was blocked and apoptotic cell death was induced by treatment with zebularine, which resulted in reduced HepG2 cell viability.

Zebularine affects HepG2 cells growth arrest and apoptosis via DNA methylation-independent pathway

Because of zebularine's activity as a DNMT inhibitor in other model systems [29,30], its effect on the expression of DNMTs in HepG2 cells was examined. As expected, zebularine treatment was associated with a statistically significant dose-dependent depletion of DNMT1, DNMT3a, and DNMT3b (Fig. 2A).

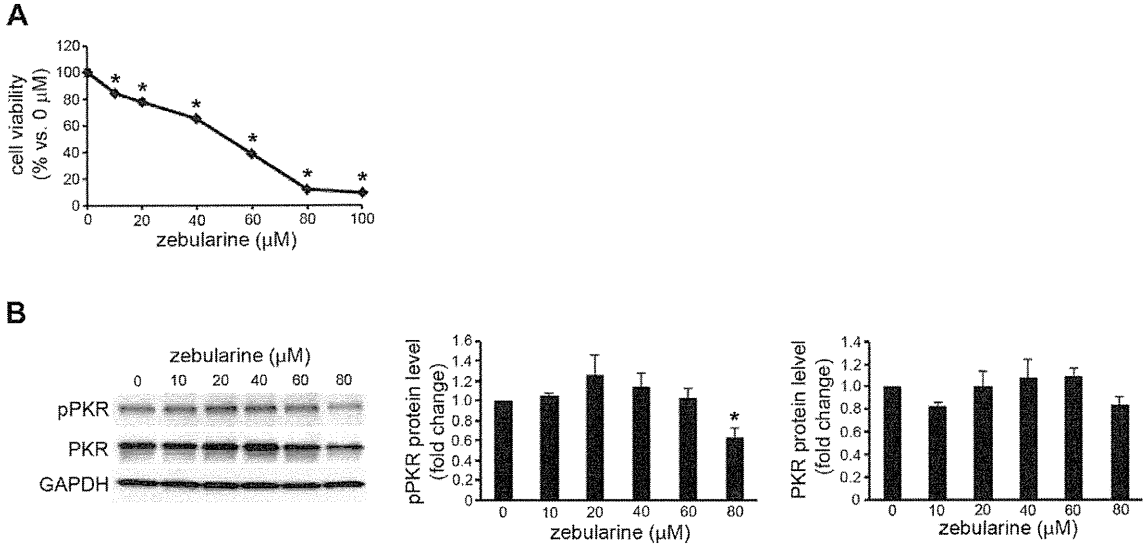

Figure 8. Effects of zebularine on phosphorylation of PKR in HeLa cells. (A) HeLa cells were treated with zebularine at indicated concentrations for 72 h. Cell growth was measured by WST assay. (B) The phosphorylation and expression of PKR after zebularine treatment for 72 h at different concentrations. After treatment, the cells were harvested and western blot analysis was performed to detect the phosphorylated and total PKR protein level. GAPDH was used as a loading control. *$p<0.05$, compared to 0 μM.
doi:10.1371/journal.pone.0054036.g008

Since zebularine decreased DNMT protein levels, to determine whether the growth inhibition and/or apoptosis induction in HepG2 cells by zebularine are a result of a change in DNA methylation, we obtained the genome-wide methylation profiles of zebularine-treated and -untreated (control) HepG2 cells using an Illumina Infinium HumanMethylation450 BeadChip (GEO accession number GSE42490). Among 482,421 assays for CpG sites, 482,260 assays fulfilled our quality control criteria (detection p value <0.01 and no missing beta value for both groups) and were subjected to the following analysis. For each assay, delta-beta value (= average of the beta values of three zebularine-treated samples − average of those of three controls) was calculated. As shown in Fig. 2B, the methylation profiles were highly similar between zebularine-treated and -untreated HepG2 cells. The number of CpG sites whose delta-beta values are >0.1 and <-0.1 was 35 and 162, respectively. At the majority (99.96%) of CpG sites, methylation levels were nearly the same under the two conditions. To further assess whether these minor methylation changes are observed at specific genes or genomic regions, we conducted region-level methylation analysis using the IMA package [28]. Among 26,659 CpG islands (CGIs), only five showed a significant change (adjusted p value <0.05 and $|\text{delta-beta value}| > 0.1$) of the methylation level upon zebularine treatment (Table S1). All five CGIs were found to be highly methylated in control HepG2 cells (beta value >0.8), and to be partially hypomethylated (delta-beta range -0.11–-0.21) in zebularine-treatment cells. One CGI is located in an intron of the AGAP1 gene that encodes ArfGAP with GTPase domain, ankyrin repeat, and PH domain 1 protein. Another CGI is located 10 kb downstream of the USP18 gene that encodes ubiquitin specific peptidase 18. The other three CGIs are not associated with any RefSeq gene structure (within 50 kb distance). It is unlikely that the slight decrease in DNA methylation at these five CGIs causes growth arrest and apoptosis in HepG2 cells. These results suggest that the administration of zebularine has little effect on DNA methylation in HepG2 cells, and that the inhibited cell growth and induced apoptosis observed in HepG2 cells upon zebularine treatment are caused by unknown mechanisms that are independent of DNA methylation.

Zebularine inhibited CDK and phosphorylation of protein retinoblastoma

To estimate the mechanism by which zebularine inhibits HepG2 cell proliferation, we investigated the change in CDK2 expression that was associated with cell-cycle regulation after zebularine treatment. Our results showed that the levels of CDK2 were downregulated in HepG2 cells at 24 h by zebularine treatment (Fig. 3). Protein retinoblastoma (Rb) plays a critical role in governing cell-cycle progression, especially for the transition from the G1 to the S phase [31], where the total and phosphorylation level of Rb was detected. Our results revealed that phosphorylated Rb (p-Rb) decreased in a concentration-dependent manner 24 h after zebularine treatment, which was accompanied by a reduction in total Rb (Fig. 3).

Zebularine increased $p21^{WAF/CIP1}$ and p53 level in HepG2 cells

Previous studies have demonstrated that tumor suppressor protein $p21^{WAF/CIP1}$ and p53 play an important role in G0/G1 arrest in HepG2 cells [32]. Therefore, in order to determine whether these two proteins play a role in inhibiting cell proliferation, the HepG2 cells were exposed to zebularine and analyzed for change on the protein level of $p21^{WAF/CIP1}$ and p53. The results showed that after 24 h of zebularine treatment, the $p21^{WAF/CIP1}$ and p53 protein level was higher in HepG2 cells than in the control (Fig. 4).

The effect of zebularine on p44/42 MAPK expression

To further clarify the mechanism of the proliferation inhibitory effect of zebularine on HepG2 cells, we examined the expression of p44/42 MAPK in HepG2 cells after zebularine treatment. As shown in Fig, 5, zebularine increased the level of phosphorylated p44/42 MAPK, whereas total p44/42 MAPK was unaffected by the zebularine treatment, as judged by comparisons with GAPDH as a loading control. This data indicates that zebularine can increase the phosphorylation of p44/42 MAPK.

Zebularine induced apoptosis via caspase pathway

To investigate whether zebularine-induced apoptosis was associated with the caspase family proteins, the activity of caspase-3/7, -8, and -9 was examined after zebularine treatment at 72 h. As shown in Fig. 6A, the activity of caspase-3/7 was significantly increased at an apoptosis-inducible concentration of zebularine. In addition to caspase-3, the activity of caspase-8 and -9 was also increased with zebularine treatment. The expression of the proapoptotic factor Bax and the antiapoptotic factor Bcl-2 was examined by western blotting. The result demonstrated that Bax expression was not affected. On the other hand, Bcl-2 expression decreased with an increasing amount of zebularine (Fig. 6B).

Zebularine decreases the activity of PKR in HepG2 cells

A previous study showed that PKR regulates the protein expression level and phosphorylation of Bcl-2 and plays an anti-apoptotic role in HepG2 cells [33]. Since zebularine can reduce the Bcl-2 protein level, we examined PKR and the phosphorylated PKR level with zebularine treatment. Our results showed that zebularine can reduce the phosphorylated PKR level; this was accompanied by a reduction in total PKR (Fig. 7A). To determine whether PKR has an anti-apoptotic effect in HepG2 cells treated with zebularine, we overexpressed the PKR gene in HepG2 cells and exposed the cells to zebularine. We found that zebularine-induced cell death was reduced by overexpression of PKR (Fig. 7B).

The effect of zebularine on the activity of PKR in other cancer cells

Zebularine also inhibits the growth of bladder cancer, breast cancer, and cervical cancer cells [29,30,34]. Since PKR is ubiquitously expressed, we examined whether zebularine decreases the activity of PKR in other cancer cells. It was recently reported that zebularine inhibits the growth of HeLa cervical cancer cells via cell-cycle arrest and caspase-dependent apoptosis [30]. We also observed that zebularine inhibited the growth of HeLa cells, which coincided with the results of the previous study (Fig. 8A). However, our results showed that cell growth inhibiting concentration of zebularine did not reduce the phosphorylated PKR and total PKR levels in HeLa cells (Fig. 8B).

Discussion

In the present study, we investigated the effect of zebularine on human hepatic carcinoma cells and the possible mechanism. To the best of our knowledge, this is the first study to demonstrate that zebularine inhibits hepatic carcinoma cell HepG2 proliferation by inducing cell growth arrest and apoptosis via intrinsic and extrinsic apoptotic pathways.

In this study, we observed that zebularine decreased the level of DNMT1, DNMT3a, and DNMT3b in HepG2 cells. These results

were similar to the reports that DNMT inhibitor induces the depletion of DNMT1, 3a, or 3b protein in human bladder, breast, and cervical cancer cells [24,30,35]. Because tight covalent complexes of zebularine and DNMT could lead to compositional change in DNMT protein, it is plausible that DNMTs can be degraded via a ubiquitination system, consequently being observed in the reduction of its expression [30]. On the other hand, our results suggest that zebularine has little effect on DNA methylation in HepG2 cells. Thus, it seems that the cell-cycle arrest and apoptosis observed in HepG2 cells upon zebularine treatment are caused by mechanisms that are independent of DNA methylation.

Eukaryotic cell proliferation is a highly regulated system that is controlled by CDK-cyclin complexes. The cell-cycle transition from the G1 to the S phase was the major regulatory checkpoint in this process. This transition is characterized by the phosphorylation of Rb, and the CDK-cyclin complex catalyzes the reaction [36,37]. In this study, we found that zebularine inhibited the CDK2 and p-Rb accompanied by a decrease in total Rb, which resulted in cell-cycle arrest and the exertion of its antiproliferative effect. Cell-cycle inhibitor $p21^{WAF/CIP1}$ plays an important role in the G1/S progression process. It may inhibit the activity of the CDK-cyclin complex to regulate cell-cycle progression. These effects can be mediated through p53-dependent or -independent machinery according to the types of stimuli [38–43]. There are two p53-binding elements located at the $p21^{WAF/CIP1}$ gene promoter that can be transactivated by the accumulated nuclear p53 after DNA damage [44]. It is reported that p53-dependent G1 growth arrest is mediated by $p21^{WAF/CIP1}$, and $p21^{WAF/CIP1}$ is the CDK inhibitory protein transcriptionally regulated by p53 [45]. Our results showed that the $p21^{WAF/CIP1}$ level was increased after zebularine treatment. In addition, zebularine also upregulated p53 protein. Thus, in the present study, both p53 and $p21^{WAF/CIP1}$ may perform their function by inhibiting the kinase activities of CDK-cyclin complexes to stimulate cell-cycle arrest, which was attributed to the zebularine effect.

MAPKs are essential components of the intracellular signal transduction pathways that regulate cell proliferation and apoptosis. One subgroup of MAPKs, p44/42 MAPK (ERK1/2), is an important target in the diagnosis and treatment of cancer and has been reported to be required for the upregulation of $p21^{WAF/CIP1}$ that results in cell-cycle arrest [46–48]. Furthermore, the high-intensity p44/42 MAPK signal leads to the repression of CDK2 kinase activity for p-Rb, which mainly regulates the proliferation of HepG2 cells [49]. In the present study, MAPK signaling pathway regulation after zebularine treatments was investigated. We found that zebularine treatment upregulated the phosphorylation of p44/42 MAPK. Therefore, it is suggested that the p44/42 MAPK pathway plays a role in zebularine-induced cell-cycle arrest by regulating the activity of $p21^{WAF/CIP1}$ and Rb.

During the process of apoptosis, caspases are essential for the initiation and execution of cell death in a self-amplifying cascade in response to various stimuli [50]. Two major apoptotic pathways have been identified: the extrinsic and intrinsic apoptotic pathways. The extrinsic pathway is activated by death receptors, which recruit initiator caspase-2, -8, or -10 through adaptor molecules, whereas the intrinsic signals result in the activation of caspase-9. These initiator caspases can sequentially cleave and activate the effector caspase (caspase-3, -6, and -7), which play an important role in mediating cellular destruction [51]. Our results showed that zebularine appeared to induce the apoptosis of HepG2 cells via the intrinsic pathway, as shown by the activation of caspase-9, and the extrinsic pathway, as shown by the activation of caspase-8, which led to caspase-3 activation. Proteins from the Bcl-2 family can be divided into two groups: suppressors of apoptosis (e.g., Bcl-2, Bcl-XL, and Mcl-1) and activators of apoptosis (e.g., Bax, Bok, Hrk, and Bad). These proteins are key regulators of the intrinsic pathway of apoptosis, setting the threshold for engagement into the death machinery [52,53]. Among these, the anti-apoptotic Bcl-2 protein acts to suppress apoptosis by preventing the release of apoptogenic proteins, such as cytochrome c, that reside in the intermembrane space of mitochondria. Functionally, Bax acts in opposition to Bcl-2 and facilitates the release of these mitochondrial apoptogenic factors by translocation and oligomerization [54–56]. Thus, the ratio of Bax/Bcl-2 determines, in part, the susceptibility of cells to death signals and might be a critical factor in a cell's threshold for apoptosis [57]. In this study, the expression of Bax and Bcl-2 proteins in zebularine-treated HepG2 cells was examined by western blot assay. We found that although Bax protein levels were not affected, Bcl-2 protein level was downregulated with zebularine treatment, which led to a marked increase in the Bax/Bcl-2 ratio and then apoptosis.

Initially identified as an antiviral protein, PKR is best known for triggering cell defense responses and initiating innate immune responses by arresting general protein synthesis and inducing apoptosis during virus infection [58]. Activated PKR, known as a eukaryotic initiation factor 2-alpha (eIF-2α) kinase, induces the phosphorylation of eIF-2α [59], which inhibits the initiation of translation through the tRNA-40S ribosomal subunit. On the other hand, PKR is involved in controlling the transcription of Bcl-2 in HepG2 cells, mediated by the transcription factor NF-κB [33]. In this study, we observed that zebularine can reduce the phosphorylation of PKR, which indicates the activated PKR. In addition, overexpression of PKR reduced zebularine-induced cell death. Thus, our results suggest that zebularine decreases the activity of PKR and results in apoptotic cell death via reduced NF-κB activity and the downregulation of Bcl-2. The fact that zebularine inhibits the growth of bladder, breast, and cervical cancer cells [29,30,34] and that PKR is ubiquitously expressed led us to hypothesize that zebularine induced the cell growth arrest via the downregulation of PKR in other cancer cells. When we examined the effect of zebularine on PKR expression in HeLa cells, we observed, however, that zebularine did not decrease the phosphorylation of PKR and the total PKR level. These results suggest that there are differences in the mechanism by which zebularine inhibits cell growth among the different types of carcinomas. The action and mechanisms of zebularine must therefore be further investigated in other cancer cells.

In conclusion, our observation indicated that zebularine inhibited cell growth and induced apoptotic cell death, which contributed to its antiproliferation effects against hepatocellular carcinoma HepG2 cells. The most likely mechanism underlying the zebularine-induced growth arrest involves an initial induction of p44/42 phosphorylation and an increase in $p21^{WAF/CIP1}$ expression, which leads to a reduction in G1-related CDKs such as CDK2 protein and p-Rb, and then ultimately arrests the HepG2 cell cycle. Furthermore, zebularine decreased the activity of PKR, and resulted in apoptotic cell death via the downregulation of Bcl-2.

Supporting Information

Table S1 List of CGIs showing a significant change in DNA methylation level upon zebularine-treatment in HepG2 cells.
(XLS)